

Cats Protecting Birds Revisited with a Spatial Approach

James Gambino¹, Marco V. Martínez-Martínez²,

Kehinde Salau³, Edmé L. Soho⁴

David E. Hiebeler⁵, Fabio Sánchez⁶,

David Murillo³

¹ Department of Applied Mathematics, Columbia University, New York, NY

² Facultad de Ciencias, Pontificia Universidad Javeriana, Bogota, Colombia

³ Department of Mathematics and Statistics, Arizona State University, Tempe, AZ

⁴ Department of Mathematical Sciences, Montclair State University, Montclair, NJ

⁵ Department of Mathematics and Statistics, University of Maine, Orono, ME

⁶ Biological Statistics and Computational Biology, Cornell University, Ithaca, NY

July 30, 2007

Abstract

The mesopredator release hypothesis (MRH) suggests that in the absence of large,

dominant predators, a population of smaller predators increases and, in the process, generates a decline in the prey community. The MRH has been used in attempts to comprehend problems involving the management of introduced species in islands and the extinction or declination of superpredators in an ecosystem due to anthropogenic pressures. The dynamics of this system were studied using a spatially explicit model with mean field and pair approximations. We included mathematical analysis of the mean field model, as well as numerical analysis for both approximations. The results of the simulation support the claims of the MRH and suggest that control of the mesopredator population is the most feasible method to ensure the persistence of endangered prey populations. Spatial modelling is a complex but valuable tool for studying such phenomena occurring in nature.

Introduction

The transformation of natural habitats to agricultural lands, hunting, climate change, introduction of alien species, and of contaminants have detrimental impacts on biodiversity [25]. One theory to understand the loss of biodiversity is the Mesopredator Release Hypothesis (MRH). MRH states that in the absence of large, dominant predators (superpredators), smaller predators and omnivores (mesopredators) undergo population explosion up to ten times their nominal level. This process generates a decline in the underlying prey community, sometimes driving them to extinction [29]. The MRH has been used in attempts to comprehend and resolve two conservation problems.

The first problem involves the management of introduced species in islands. These alien

species are a major contributor to the extinction of native species in island ecosystems [3]. In general, these adaptable species are successful in their new ecosystem because the community of native species does not possess the evolutionary history to respond to this new interaction. Furthermore, these alien species encounter relatively few pathogens and parasites [12]. Alien predators are a major threat to 40% of endangered island bird species, with feral cats (*Felis catus*) and mongooses (*Hagolestes auropunctatus*) among the most notorious and harmful of the introduced predators [18]. Feral cats have been introduced into at least 65 island groups where they are responsible for the loss of many large land and seabird colonies, populations, or even species [22, 19]. Cats also constitute a major threat to many endemic reptile and mammal species [17, 4, 30].

Programs geared towards controlling the population of cats and other alien predators are largely recognized as the best way to restore ecosystems. Although eradication of these alien cat populations has often been attempted, only a few have been successful, and several are still being evaluated [13]. One reason for the abortiveness of these programs is the simultaneous introduction of the predator and prey. Many islands have both alien cats and alien rats. Rats have an extremely deleterious effect on many organisms such as amphibians, reptiles, birds and mammals [2, 8]. This effect can be indirect, by competition for food, shelter or nest-sites [28]; or direct, by predation of eggs, chicks, juveniles and even adult ground-nesting seabirds, land birds and tree-nesting birds [1]. In this case, the removal of the cat population, the top predators, has caused a surge in the rodent population and may still lead to the extinction of the bird population. In some particular situations supporting the MRH, the presence of a

controlled population of cats might be, at least temporarily, more beneficial to the endemic existence of the prey, since the cats maintain the population of rats at low levels. Although the cats also prey on the endangered species, the beneficial effects of reducing the population of rats are superior relative to the damage done by predation to the endemic species [32, 7].

The second problem is the extinction or declination of superpredators in an ecosystem due to fragmentation (e.g. urbanization), predator suppression (e.g. hunting), and the conversion of natural habitats to agricultural lands [26]. In areas of Midwestern North America and Coastal Southern California, where the aforementioned land conversions and predator suppressions have occurred, the population of coyotes has severely decreased over the past century [9, 26]. These areas have also seen an increase in the population of small predators including raccoons, foxes, and possums, a plausible result of declining predation against these mammals. Raccoons are a preferred prey among coyotes, so the absence of these top predators is a plausible explanation for the drastic increase in the population of smaller predators [23]. However, increased numbers of raccoons and other small predator populations could lead to, and in many cases may have already led to, increased predation on the ground-nested bird population as suggested by the MRH. Could a controlled population of coyotes restore the stifling bird populations in these problematic U.S. regions? Studies in the prairie pothole region of North America and the Chaparral ecosystem of California found there are more flourishing bird populations in areas with coyotes as opposed to areas without them [23]. While these studies do not prove the existence of the MRH, they certainly support the claim.

The MRH is considered a possible explanation for the decline and extinction of prey species

[29, 23, 15]. However, this claim is difficult to verify for logistic, financial and ethical reasons [9]. Instead, scientists utilize mathematical models and simulations to assess the validity of the MRH or propose possible management strategies. A mathematical study by Courchamp et. al [7] concluded the MRH is plausible and the hasty removal of top predators could very well lead to the extinction of prey via the rise in mesopredator density. A more recent study by Fan et. al. [14] concluded that although there are cases where rapid growth of the mesopredator leads to the eventual extinction of the prey, under certain nontrivial conditions the prey population is stifled by the mesopredator release but do not go extinct.

Previous models lack explicit spatial considerations. There are many examples which indicate spatial considerations facilitate the persistence of populations in nature [24]. This phenomenon is prevalent in many applications including host-pathogen [33], plant-pollinator [34] and predator-prey [20] systems.

In this paper we first introduce the general model we used in our analysis of the mesopredator release (Section 1), then we examine a pair approximation (Section 2) and the mean field approximation (Section 3). We then introduce the numerical solutions to the approximation (Section 4) followed by a description of the actual simulation (Section 5). Finally, we conclude with our results (Section 6).

1 Model

We need a model that would adequately represent the three-species mesopredator system while taking into account a spatial environment, we develop a stochastic spatial temporal model

using a spatially discrete lattice and continuous time. It is important to address the relation of these species because spatial arrangement affects the interactions between them. In particular, clustering, when a single species densely populates a convex domain within the lattice, is an important result of spatial arrangement. For example, when prey are clustered, predators only have access to the perimeter of the clusters and not the entire prey population. Each site on the lattice contains an integer value as described in Table 1. The model has eight possible events that can occur on the lattice.

States	Description
0	Empty Site
1	Site contains a Prey
2	Site contains a Mesopredator
3	Site contains a Superpredator

Table 1: Lattice States and Description

These states disperse onto the lattice creating a spatial environment where events may occur. The events are defined by a list of eleven parameters given in Table 2. While most of the parameters are intuitive a few warrant a more detailed explanation:

- ϕ_i with $i = 1, 2, 3$ is the intrinsic birth rate for the prey, mesopredator and superpredator respectively. We assume that their dispersal is local meaning the parent site gives birth to adjacent lattice sites. Realistically, there should be a delay between birth and a new

Parameters	Description	SIM Values	PA Values	MF Values
ϕ_1	prey birth rate	5	9	9
ϕ_2	mesopredator birth rate	12	7	6
ϕ_3	superpredator birth rate	0	0	0
μ_1	prey death rate	$\frac{1}{7}$	2	2
μ_2	mesopredator death rate	$\frac{1}{2}$	1.5	1.5
μ_3	superpredator death rate	$\frac{1}{10}$.3	.3
ν_2	mesopredator foraging rate	1.2	6	5
ν_3	superpredator foraging rate	50	10	10
η_2	probability that successful meso- predator predation leads to birth	.6	.6	.5
η_{31}	probability that successful su- perpredator predation on prey leads to birth	.02	.15	.15
η_{32}	probability that successful su- perpredator predation on meso- predator leads to birth	.04	.35	.35

Table 2: Model parameters with simulation (SIM), pair approximation (PA), and mean field (MF) values.

site being occupied but for reasons of simplicity we have ignored that effect. Thus ϕ_i is a per capita birth rate.

- ν_j with $j = 2, 3$ is the foraging rate of the mesopredator and superpredator respectively. We assume the predator can only search for food within its von Neuman neighborhood (i.e. four orthogonal neighbors) and that it is equally likely to choose any neighbor. Thus, the predation rate in any given direction is $\frac{\nu_j}{4}$. We also make the assumption that once a foraging predator locates a prey site, it will consume the prey on that site.
- η_2 is the probability that prey consumption by the mesopredator leads to the birth of a new mesopredator. Once a mesopredator forages successfully and consumes a prey, with probability η_2 it will give birth onto the site that previously contained the prey. It is important to note that this process is considered one event; and so a 1-site can become a 2-site in one timestep.
- η_{3k} with $k = 1, 2$ is the probability that the consumption of prey ($k = 1$) or mesopredator ($k = 2$) by the superpredator leads to the birth of a new superpredator. After consumption of the k-site occupant, the superpredator gives birth on the site with probability η_{3k} ; and this is considered one event.

The summary of possible transitions between states for single sites are as described in Table 3.

- State [0]: State [1], [2], [3] can become State [0] if a prey, mesopredator, or superpredator dies of non-predatory causes. In addition, states [1] and [2] can become state [0] if they

[1][2][3]	\Rightarrow	[0]
[0]	\Rightarrow	[1]
[0][1]	\Rightarrow	[2]
[0][1][2]	\Rightarrow	[3]

Table 3: Possible state transitions

are consumed but no immediate predator reproduction occurs.

- State [1]: State [0] can become state [1] if a prey is born into the site.
- State [2]: State [0] can become state [2] if a mesopredator is born into the site. State [1] can become state [2] if a mesopredator consumes a prey and then reproduces at the site.
- State [3]: State [0] can become state [3] if a super predator is born into the site. States [1] and [2] can become state [3] if a superpredator consumes a prey or mesopredator and then reproduces at the site.

2 Pair Approximation

Pair approximation is a modeling technique which allows for the introduction of local or long distance spatial interaction in a mathematical model. With pair approximation, it is assumed that two nonadjacent sites are independent, given that the state of their common neighbor is known. The pair approximation model contains a set of differential equations which describe the configuration of pairs of sites through the probability of the variations of states. The state

variables are $p[ij]$, the probability that for a pair of adjacent sites chosen at random from the lattice, the first is in state i and the second is in state j . Pair approximation models are usually more accurate than the regular approach of spatially implicit mean field approximations. The pair approximation models assume spatial symmetry without consideration of the directional orientation (North, South, East, and West), such that for any two states a and b , the probabilities $p[ab]$ and $p[ba]$ would be the same. Throughout this paper, we will assume complete spatial symmetry, in particular rotational symmetry, i.e.,

$$p[ij] = p[ji] = p \begin{bmatrix} i \\ j \end{bmatrix} = p \begin{bmatrix} j \\ i \end{bmatrix},$$

for i and j equal to 0, 1, 2, or 3. To construct the pair approximation equations, the different attainable configurations of pairs of sites were examined with their transitions. There are four states with sixteen possible pairs. The assumption of spatial symmetry allows for the reduction of the sixteen possible pairs, since $p[01] = p[10]$, $p[13] = p[31]$, to ten.

Also, all the probabilities must sum to 1 hence, $p[00] + 2p[01] + 2p[02] + 2p[03] + p[11] + 2p[12] + 2p[13] + p[22] + 2p[23] + p[33] = 1$. A marginal single site probability can be computed by summing over all the possible ways a site can be in a given state and its neighbour in any other state. In the case of our model,

$$p[1] = p[10] + p[11] + p[12] + p[13].$$

We also define $Q_{j|i}$ to be the conditional probability that a site has a neighbor in state j given that it is in state i . Thus,

$$Q_{j|i} = \frac{p(\text{my neighbor is } j \text{ AND I am } i)}{p(\text{I am } i)} = \frac{p[ij]}{p[i]}.$$

In order to obtain the diagram used to construct the pair approximation equations as shown in Figure 1, one must verify each of the state variables separately. The main purpose is to demonstrate that the transitions are allowed, given that only one event can occur at a time. The full nine equations are contained in Appendix A.

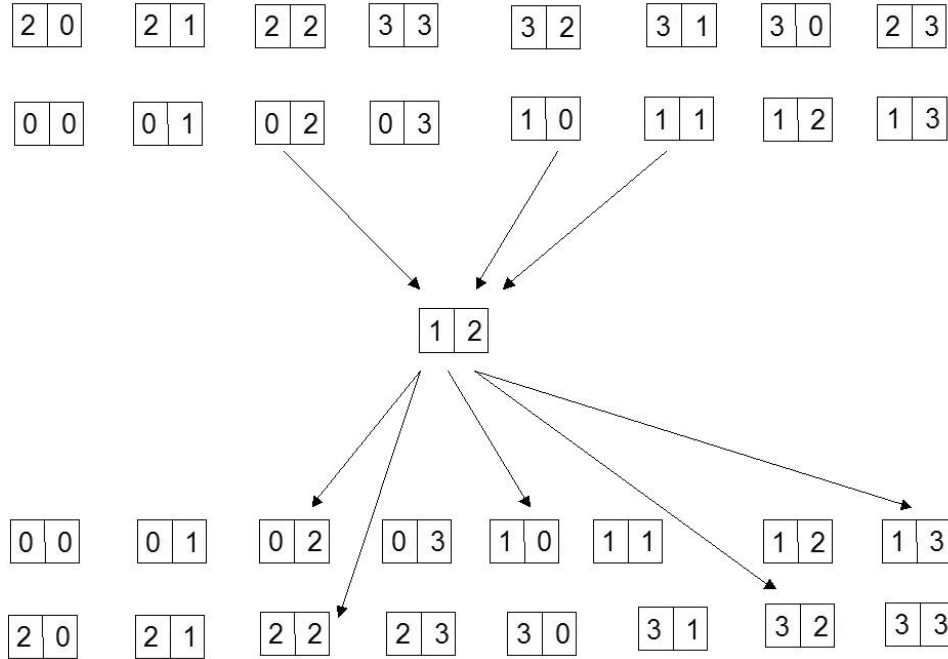


Figure 1: This figure demonstrates the inflow of possible pairs of states that can turn into pair [12] and the outflow of states that [12] can turn into during a single event via the direction of the arrows.

3 Mean Field Approximation

3.1 Definition

The mean field approximation is a method of using systems of differential equations to express changes in the proportion of states on a lattice. One assumption of the mean field approximation is that the population is well mixed, and so space is invariant in the dynamics of the model. In the mean field approximation $p[i]$ represents the probability that a randomly-chosen site is in state i . To write out the differential equation for each variation of state, we base it on the main equation:

$$\frac{dp[i]}{dt} = \underbrace{\sum_{j \neq i} p[j] r_{j \rightarrow i}}_a - p[i] \underbrace{\sum_{j \neq i} r_{i \rightarrow j}}_b,$$

with a defined as sum of (other state probabilities) * (rates at which they transition into state i) and b as sum of transition rates out to all other states.

This produces the following system of nonlinear differential equations:

$$\begin{aligned} \frac{dp_0}{dt} = & \mu_1 p_1 + \mu_2 p_2 + \mu_3 p_3 + \nu_2 (1 - \eta_2) p_2 p_1 + \nu_3 (1 - \eta_{31}) p_3 p_1 \\ & + \nu_3 (1 - \eta_{32}) p_3 p_2 - (\phi_1 p_1 + \phi_2 p_2 + \phi_3 p_3) p_0 \end{aligned} \quad (1)$$

$$\frac{dp_1}{dt} = \phi_1 p_1 p_0 - (\mu_1 + \nu_2 p_2 + \nu_3 p_3) p_1 \quad (2)$$

$$\frac{dp_2}{dt} = \phi_2 p_2 p_0 + \nu_2 \eta_2 p_1 p_2 - (\mu_2 + \nu_3 p_3) p_2 \quad (3)$$

$$\frac{dp_3}{dt} = \phi_3 p_3 p_0 - \mu_3 p_3 + \nu_3 p_3 p_1 \eta_{31} + \nu_3 p_3 p_2 \eta_{32}. \quad (4)$$

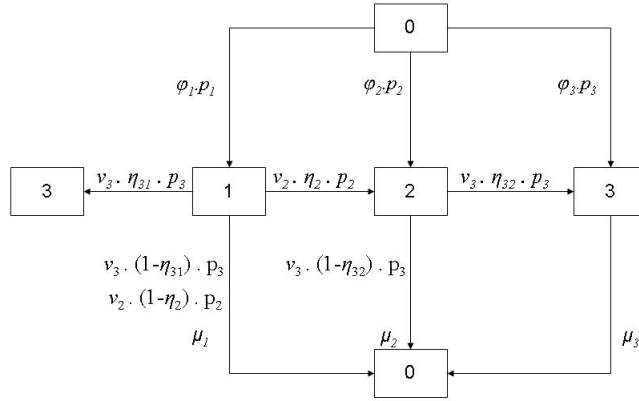


Figure 2: The mean-field flow chart. We duplicate the states 0 and 3 so as not to complicate the flow chart with intersecting arrows.

We could also write down the equation for $\frac{dp_0}{dt}$, but since all the probabilities must sum to 1, i.e.

$$\frac{dp_0}{dt} + \frac{dp_1}{dt} + \frac{dp_2}{dt} + \frac{dp_3}{dt} = 0,$$

then we can replace p_0 by $1 - p_1 - p_2 - p_3$ in equations 2-4. Therefore, three equations are sufficient to describe the system.

3.2 Equilibria and Stability

Solving equations (2-4) for the three species yields eight potential steady states. We found explicit expressions for all equilibria and their biological implications (see Table 4). To determine

whether the equilibria are locally asymptotically stable (L.A.S.) we use linearization via the Jacobian:

$$\begin{bmatrix} \Lambda\phi_1 - p_1\phi_1 - \mu_1 - \nu_2p_2 - \nu_3p_3 & -p_1\phi_1 - p_1\nu_2 & -p_1\phi_1 - p_1\nu_3 \\ -p_2\phi_2 + \eta_2\nu_2p_2 & \Lambda\phi_2 - p_2\phi_2 + \eta_2\nu_2p_1 - \mu_2 - \nu_3p_3 & -p_2\phi_2 - p_2\nu_3 \\ -p_3\phi_3 + \eta_3\nu_3p_3 & -p_3\phi_3 + \eta_3\nu_3p_1 & \Lambda\phi_3 - p_3\phi_3 + \eta_3\nu_3p_2 - \mu_3 \end{bmatrix}$$

with $\Lambda = 1 - p_1 - p_2 - p_3$. A sufficient condition for the existence of these steady states is that $0 \leq p_i \leq 1$, since p represents a proportion of sites.

Notation	Description
E_0	Species-free equilibrium
E_i	The persistence of only species i with $i = 1, 2, 3$
E_{ij}	The persistence of species i and j with $i, j = 1, 2, 3$ and $i \neq j$
E_{123}	The coexistence of all species

Table 4: Equilibria have the form $E = (p_1^*, p_2^*, p_3^*)$ where p_i^* is the equilibrium value of species i .

Even-though the equilibria for the coexistence of species can be computed, we could derive simple conditions for L.A.S. for E_{12} , E_{13} , E_{23} , or E_{123} .

- $E_0 = (0, 0, 0)$.

This is the species-free equilibrium and the proportion of empty sites is exactly equal to one. This is also referred to as the trivial steady state. The Jacobian matrix evaluated

at the species-free equilibrium yields the corresponding eigenvalues

$$\phi_1 - \mu_1,$$

$$\phi_2 - \mu_2,$$

$$\phi_3 - \mu_3.$$

And so the conditions for local stability at this equilibrium point are satisfied when all three eigenvalues are less than zero; thus,

$$\frac{\phi_1}{\mu_1} < 1,$$

$$\frac{\phi_2}{\mu_2} < 1,$$

$$\frac{\phi_3}{\mu_3} < 1.$$

If the intrinsic birth rate of the prey is less than its death rate then it will eventually die out. If that is the case, the mesopredators must rely solely on their intrinsic birth rate and if it is smaller than their death rate then they will also go extinct. With no prey or mesopredators to consume, the superpredator survives only on its own intrinsic birth rate, if its death rate surpasses its birth rate then finally it will go extinct also. And so, having the birth rates less than the death rates are sufficient conditions for the L.A.S of the species-free equilibrium.

- $E_1 = \left(1 - \frac{\mu_1}{\phi_1}, 0, 0\right)$.

This denotes the persistence of the prey population in the absence of the mesopredator and superpredator populations. This steady state is valid when $\mu_1 < \phi_1$. In order for the

prey population to persist while the other two species are nonexistent, its intrinsic birth rate must be greater than its natural death rate.

The eigenvalues for this steady state are:

$$\begin{aligned}\lambda_{11} &= -\phi_1 + \mu_1 \\ \lambda_{12} &= \frac{-\phi_1\mu_2 + \phi_2\mu_1 + \nu_2\eta_2\phi_1 - \nu_2\eta_2\mu_1}{\phi_1} \\ \lambda_{13} &= -\frac{\phi_1\mu_3 - \phi_3\mu_1 - \nu_3\eta_{31}\phi_1 + \eta_{31}\nu_3\mu_1}{\phi_1}\end{aligned}$$

this steady state is L.A.S. when the following necessary conditions hold

$$\begin{aligned}\frac{\phi_1}{\mu_1} &> 1, \\ \frac{\phi_2}{\mu_2} &< 1, \\ \frac{\phi_3}{\mu_3} &< 1.\end{aligned}\tag{5}$$

So, the birth rate of the prey must be greater than its death rate, which also follows from the existence of this steady state. Furthermore, the intrinsic birth rates of both the mesopredator and the superpredator must be less than their death rates.

- $E_2 = \left(0, 1 - \frac{\mu_2}{\phi_2}, 0\right)$.

This is the persistence of the mesopredator population in the absence of the prey and superpredators. The steady state is biologically significant when $\mu_2 < \phi_2$. The intrinsic birth rate of the mesopredator must exceed its natural death rate for it to survive in the absence of prey or superpredators. This condition is feasible since mesopredators do not rely on the availability of a specific prey for sustenance.

The corresponding eigenvalues are,

$$\begin{aligned}\lambda_{21} &= -\frac{-\phi_1\mu_2 + \phi_2\mu_1 - \nu_2\mu_2 + \phi_2\nu_2}{\phi_2} \\ \lambda_{22} &= -\phi_2 + \mu_2 \\ \lambda_{23} &= -\frac{\phi_2\mu_3 - \nu_3\eta_{32}\phi_2 + \nu_3\eta_{32}\mu_2 - \phi_3\mu_2}{\phi_2}\end{aligned}$$

and it is L.A.S. when the following necessary conditions are met:

$$\begin{aligned}\frac{\phi_2}{\mu_2} &> 1, \\ \phi_1\frac{1}{\mu_1 + \nu_2} &< \frac{\phi_2}{\mu_2} \\ \frac{\phi_3}{\mu_3} &< 1.\end{aligned}\tag{6}$$

So, the birth rate of the mesopredator must be greater than its death rate so loss of the prey does not negatively affect the species. The death rate of the superpredator must exceed its birth rate. Lastly, the number of offspring produced by the prey before natural death or death via mesopredator predation must be less than the number of offspring produced by a mesopredator before its death.

- $E_3 = \left(0, 0, 1 - \frac{\mu_3}{\phi_3}\right)$.

This is the existence of the superpredator population without any prey or mesopredators in the environment. This steady state is viable if the intrinsic birth rate of a superpredator is larger than its death rate. Sole existence of the superpredators is practicable for the same

reason as that of the mesopredators; their survival is not dependent on the availability of a specific mesopredator or prey.

The corresponding eigenvalues are

$$\begin{aligned}\lambda_{31} &= \frac{\phi_1\mu_3 - \phi_3\mu_1 + \nu_3\mu_3 - \phi_3\nu_3}{\phi_3} \\ \lambda_{32} &= \frac{\phi_2\mu_3 - \phi_3\mu_2 + \nu_3\mu_3 - \phi_3\nu_3}{\phi_3} \\ \lambda_{33} &= \mu_3 - \phi_3.\end{aligned}$$

E_3 is L.A.S. when the following necessary conditions are met:

$$\begin{aligned}\frac{\phi_3}{\mu_3} &> 1, \\ \phi_1 \frac{1}{\mu_1 + \nu_3} &< \frac{\phi_3}{\mu_3} \\ \phi_2 \frac{1}{\mu_2 + \nu_3} &< \frac{\phi_3}{\mu_3}.\end{aligned}\tag{7}$$

The intrinsic birth rate of the superpredator must be greater than its death rate, so it can survive without the prey or mesopredator. Also, the number of offspring produced by the prey or mesopredator before natural death or death via superpredator predation must be less than the number of offspring produced by a superpredator before its death.

- $E_{12} = \left(\frac{\mu_2\phi_1 - \phi_2\mu_1 + \nu_2\mu_2 - \phi_2\nu_2}{\nu_2(-\phi_2 + \eta_2\phi_1 + \nu_2\eta_2)}, \frac{-\mu_2\phi_1 + \nu_2\eta_2\phi_1 + \phi_2\mu_1 - \nu_2\eta_2\mu_1}{\nu_2(-\phi_2 + \eta_2\phi_1 + \nu_2\eta_2)}, 0 \right).$

$p_1 + p_2 \leq 1$ is a sufficient condition for existence. E_{12} represents the prevalence of the prey and mesopredator populations in the absence of the superpredators. The existence

of this steady state is reliant on several necessary conditions:

$$\begin{aligned}
\frac{\phi_1}{\mu_1} &> 1, \\
\frac{\eta_2\nu_2}{\mu_2} &< 1 < \frac{\phi_2}{\mu_2}, \\
\frac{\phi_2}{\mu_2} &< \frac{\phi_1}{\mu_1}.
\end{aligned} \tag{8}$$

In effect, the birth rate of the prey must be greater than its death rate if it is to survive at all. The birth rate of the mesopredator is greater than its death rate, and both those rates exceed its birth rate from predation. So the mesopredator relies on other food sources for growth. Furthermore, (8) says that the number of offspring produced by the mesopredator before death must be less than the number of offspring produced by the prey before its death.

- $E_{13} = \left(\frac{\mu_3\phi_1 - \phi_3\mu_1 + \nu_3\mu_3 - \phi_3\nu_3}{\nu_3(\eta_{31}\phi_1 + \nu_3\eta_{31} - \phi_3)}, 0, \frac{-\mu_3\phi_1 + \phi_3\mu_1 + \nu_3\eta_{31}\phi_1 - \mu_1\nu_3\eta_{31}}{\nu_3(\eta_{31}\phi_1 + \nu_3\eta_{31} - \phi_3)} \right).$

with

$$p_1 + p_3 \leq 1.$$

This expression indicates the prevalence of only the prey and superpredator populations.

The existence of this steady state is dependent on the following conditions:

$$\begin{aligned}
\frac{\phi_1}{\mu_1} &> 1, \\
\frac{\eta_{31}\nu_3}{\mu_3} &< 1 < \frac{\phi_3}{\mu_3}, \\
\frac{\phi_3}{\mu_3} &< \frac{\phi_1}{\mu_1}.
\end{aligned} \tag{9}$$

Essentially, the prey-superpredator relationship in this case is analogous to that of prey-mesopredator in E_{12} .

- $E_{23} = (0, \frac{\phi_2\mu_3 - \mu_2\phi_3 + \nu_3\mu_3 - \phi_3\nu_3}{\nu_3(\eta_{32}\phi_2 + \nu_3\eta_{32} - \phi_3)}, \frac{-\phi_2\mu_3 + \nu_3\eta_{32}\phi_2 - \nu_3\eta_{32}\mu_2 + \mu_2\phi_3}{\nu_3(\eta_{32}\phi_2 + \nu_3\eta_{32} - \phi_3)})$.

and

$$p_2 + p_3 \leq 1.$$

This term signifies the coexistence of mesopredator and superpredator only. For existence of this equilibrium, the following conditions are necessary:

$$\begin{aligned} \frac{\phi_2}{\mu_2} &> 1, \\ \frac{\eta_{32}\nu_3}{\mu_3} &< 1 < \frac{\phi_3}{\mu_3}, \\ \frac{\phi_3}{\mu_3} &< \frac{\phi_2}{\mu_2}. \end{aligned} \tag{10}$$

Similarly, the mesopredator-superpredator relationship in this case is similar to the previous two cases; the mesopredator now acts as the prey.

- $E_{123} = (p_1^*, p_2^*, p_3^*)$. Though, the coexistence equilibrium of all three species can be computed, resolving sufficient and biologically-explainable conditions for its existence and stability is complex, therefore analysis of this state will not be included.

4 Numerical Analysis

We numerically integrate equations 2-4, the mean field model, and equations 11-19, the pair approximation model using an explicit Dormund-Prince pair (4,5) Runge-Kutta formula (ode45 in MATLAB). Figures 3 and 4 illustrate numerical solutions to the mean field model and the pair approximation model respectively.

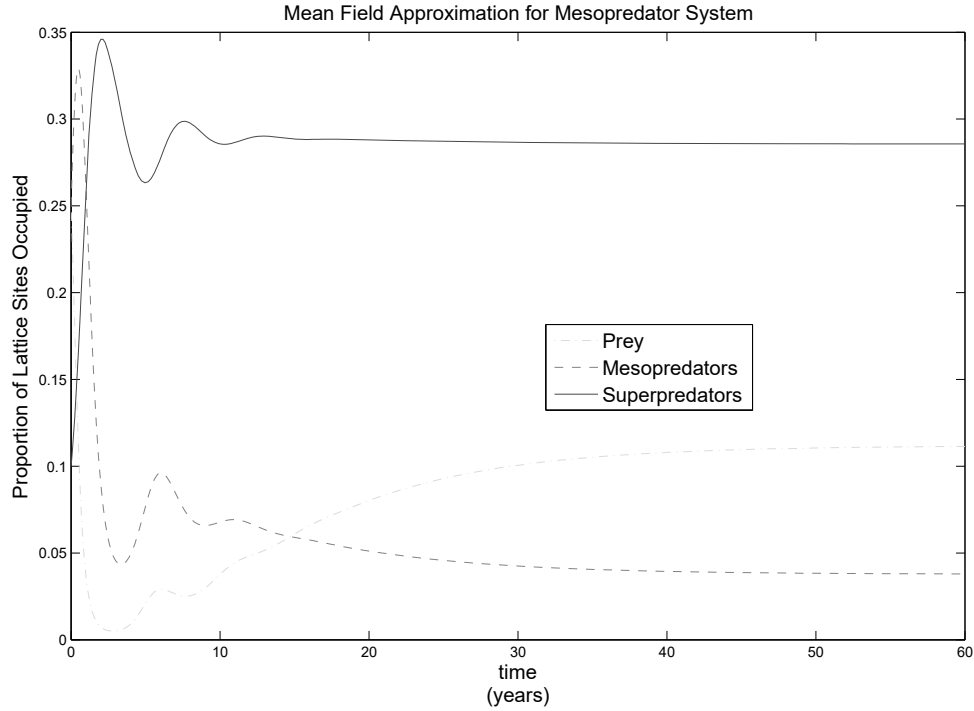


Figure 3: Mean field equations numerically integrated with parameters found in Table 2 under MF values.

In the mean field model the mesopredator and superpredator populations rise initially and then begin to decline as prey becomes scarce and they can no longer supplement their natural birth rate with additional births from predation. The prey population declines initially and then rises to a steady state which depends on the particular set of parameters in Table 2. For the two predator species there are some damped oscillations before reaching a stable equilibrium. In the pair approximation model we see the same qualitative behavior but the oscillations are more damped. While there is also coexistence in this model the numerical value of the species population at equilibria differs from that of the mean field model.

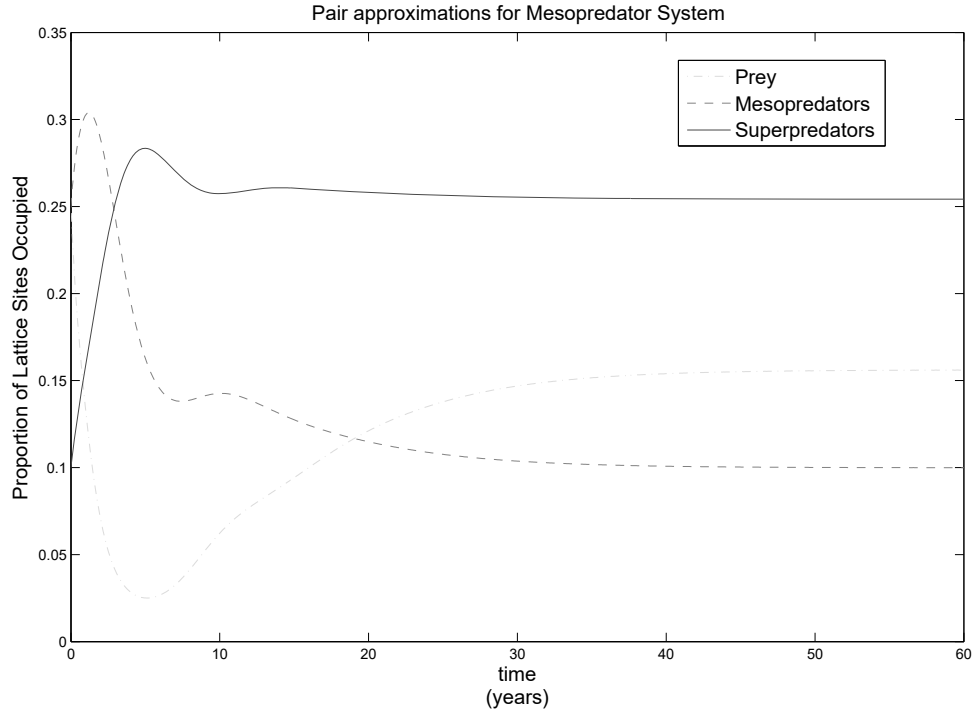


Figure 4: Pair Approximation equations numerically integrated with parameters found in Table 2 under PA values.

5 Simulation

We construct an $L \times L$ lattice, where L is an integer, using toroidal periodic boundary conditions i.e. we use wrap around boundary conditions. Next, we decide on the initial distribution of prey, mesopredators and superpredators. The initial distribution is assumed to be uniformly random across the lattice. See figure 5 for the realisation of the spatial simulation for the coexistence of all three-species.

The process is modeled by randomly choosing one of eight events: birth and death events for all three species and predation events for the two predator species. Depending on the event

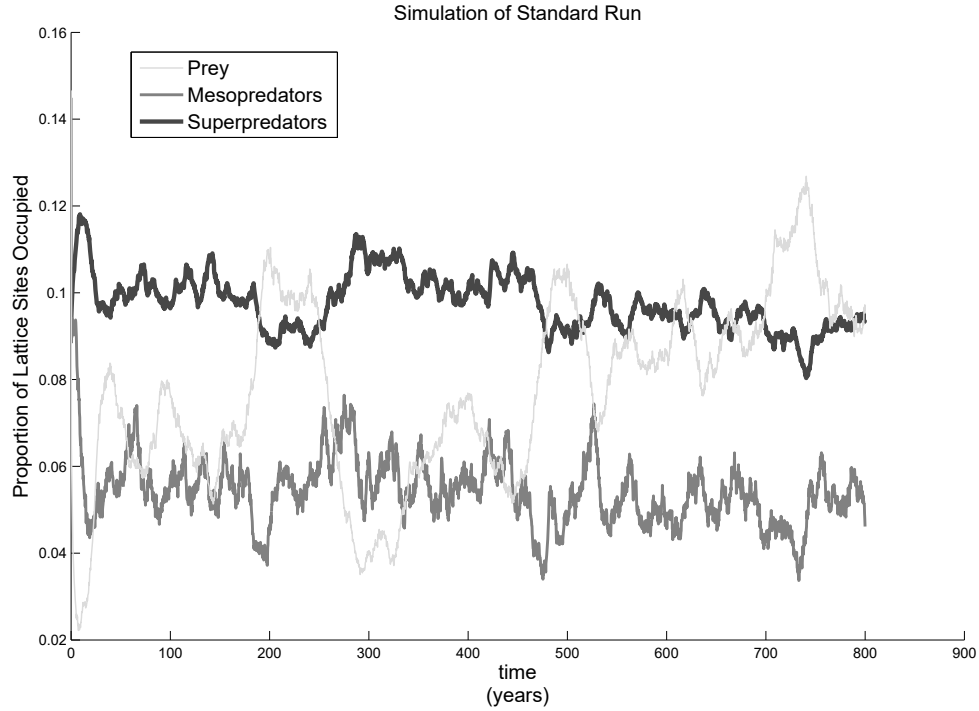


Figure 5: This is a single realization of the the spatial simulation on a 100×100 lattice. We use the simulation parameter values from Table 2 under SIM values.

chosen a cell containing a species of the appropriate type is selected at random. For example, upon selection of a superpredator predation event, a superpredator is randomly chosen from the list of superpredator sites. Then, the superpredator randomly chooses one of its neighboring sites; if the neighboring site is occupied by a prey or mesopredator the superpredator will consume it and then randomly determine whether to leave the site empty or produce a new superpredator. The lattice may be produced visually as a grid with each cell set to a specific value designating one of the 4 states.

We track the pair of lattice coordinates of all four states, as well as, the index of each pair

of coordinates in the coordinate list. The importance of bookkeeping all 10,000 cells becomes evident as only certain states can transform into others and the nearby presence of particular states affect how these transitions can occur. For example, a prey may become an empty site if it naturally dies or if a nearby predator consumes it and does not populate the site. At the end of every event we update the lattice of current values, coordinate list and lattice of indices. The population count of each species is also updated after each event. A check is made to see if enough time has passed or events have occurred and the population for each species is then recorded to lists that can be plotted at the end of the simulation. After each event two final checks are made. First, we check to see if all the species populations are zero; if so we end the simulation. Second, we check to see if the lattice has reached equilibrium. To do this, we perform a linear regression on each of the last 100 recorded population proportions versus time. If the absolute value of the slopes on all three regressions are below the set threshold of 5×10^{-4} , then we conclude that the simulation has reached equilibrium. This test for equilibria follows the method used by Caswell and Etter [5].

In our program we code rules for each type of events as follows:

- Birth of any of the species is a local event, meaning a populated site can only give birth onto one of its empty neighbors. A birth event is carried out by first selecting a member of the species and then randomly choosing one of its 4 cardinal neighboring sites. If the site is empty then the birth takes place, if not then the birth attempt is wasted.
- Natural death of any species always leaves a site empty. A death event is carried out by randomly choosing a member of the given species and then removing it from the lattice.

- Mesopredator predation is a local event. A mesopredator predation event is carried out by first selecting a mesopredator and then choosing one of its neighbors; if the neighbor is a prey then the mesopredator consumes the prey, otherwise the attempt is wasted. After consumption, the mesopredator randomly determines whether or not to populate the site with a new mesopredator.
- Superpredator predation is also a local event. During a superpredator predation event, a superpredator is randomly chosen from the list of superpredator sites. Then, the superpredator randomly chooses one of its neighbors, where neighbor is defined using Von Neumann neighborhood. If the neighboring site is occupied by a prey or mesopredator then the superpredator will consume it and then randomly determine whether to leave the site empty or produce a new superpredator.

(The MATLAB code can be obtained from any of the authors.)

5.1 Parameter Estimation

To validate the behavior of our model we want to estimate parameter values with biological significant. In order to accomplish this, we conducted an extensive bibliographical search and contacted some experts in the area. In the case of ϕ_1 , we utilize the results of Curry [10] for the species *Nesomimus spp.* He measured the number of clutches, number of eggs and the percent of hatches per year, during four years in the Galapagos (tables 1,2 and 3, respectively, [10]). We take the product of these three average (3.25%, 3.92% and 41%) to calculate ϕ_1 which is 5.22%.

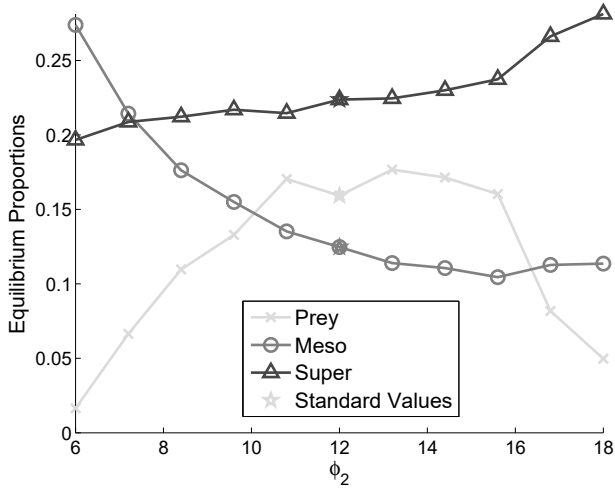
For ϕ_2 , we use the values from the Tamarin and Malecha [31] report for *Rattus rattus*; 2.3 litters per year, 5.1 embryos per litter and a final yearly production of 11.8. We also use the results from Jackson (1962) [cited in Tamarin and Malecha 1972]; 3.2 litters per year, 3.8 embryos per litter and a yearly production of 12.2. The combination of these two yearly productions yields an average of 12 rats per year. In order to calculate ϕ_3 , we assume cats cannot reproduce without predation giving $\phi_3 = 0$; this is feasible because we know these animals reproduce only when they have sufficient resources [16]. In addition, field work shows that the birth rate of cats (*Felis catus*) is small; it is in the order of 1.5 kittens per year [27]. We determine the mortality rates for each of the three species by inverting their lifespan; birds live up to 7 years [11], rats live up to 2 years [16] and we calculate an average between free-ranging cats (5) and domestic cats (15) [21] to have a lifespan of 10 years.

6 Results and Discussion

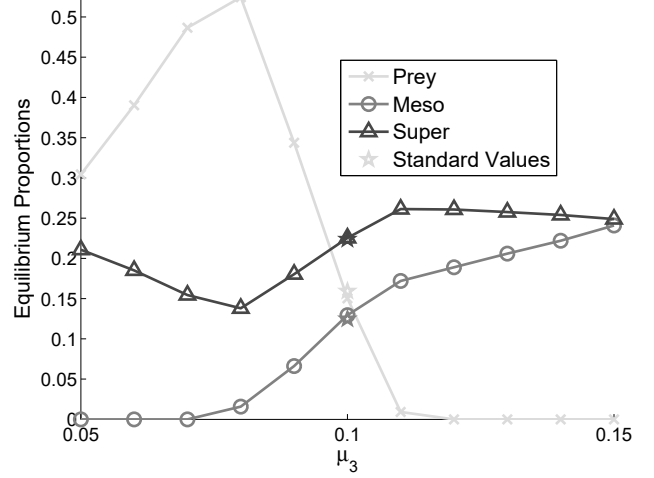
We divide our results into three primary sections. Section 6.1 will discuss our results with respect to parameter variation. Section 6.2 reveals our findings from the simulations' spatial environment and their implication. Finally, in Section 6.3 we address how our results differ from previous approaches to the mesopredator release.

6.1 Parameter Results

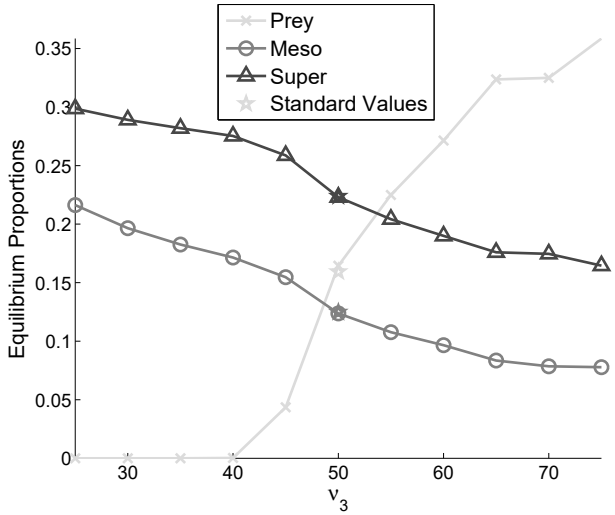
In order to better understand our model, we compute the variation of the final equilibria with respect to each of the parameters (for graphs of all of the parameters see Appendix B). Figure



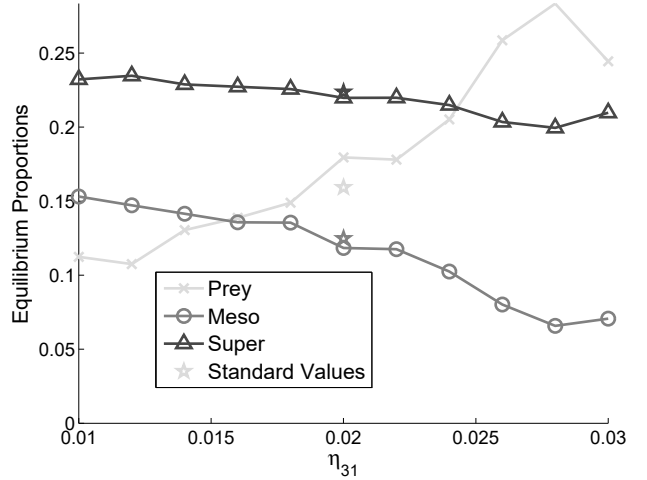
(a)



(b)



(c)



(d)

Figure 6: Plots of simulation equilibria where each point is the average of the last 100 values of the run over four key parameters on a 300×300 lattice: ϕ_2 (a), μ_3 (b), ν_3 (c), η_{31} , (d)

6 displays the dynamics that occur as a result of parameter variation. Figure 6(a) shows the final values of each species for the simulation as we vary ϕ_2 . The initial increase of ϕ_2 has a

deleterious effect on the rat population, this is because as the density of the rats increase on the lattice, the cats are able to eat more rats and, as a result, produce more cats. The bird population grows as a result of the declination in the number of rats. When the rat population reaches a low threshold, and as ϕ_2 continues to increase, the population size of birds oscillates around a maximum for some range of ϕ_2 . At this point, birds are the most populous prey for the cats on the lattice, and so the cats consume more of them; thereby allowing for an increase in the rat population due to available lattice space. As the population of rats stabilizes and the cats continue to grow, the bird population suffers a significant decline. In conclusion, the amplification of ϕ_2 is more beneficial for the cat population as opposed to the rat population.

Figure 6(b) shows the resulting change in coexistence for the three species as we vary μ_3 . Increasing μ_3 shows an initial decline in the population of cats; this allows for an increase in the number of birds and an eventual increase in the rat population as a result of less predation. The increase in the number of rats allows for the survival and later increase in the cat population. Now, with both predator populations on the rise, the birds suffer a dramatic decline in quantity. Essentially, increasing the death rate of the cats could have a deadly effect on the population of birds.

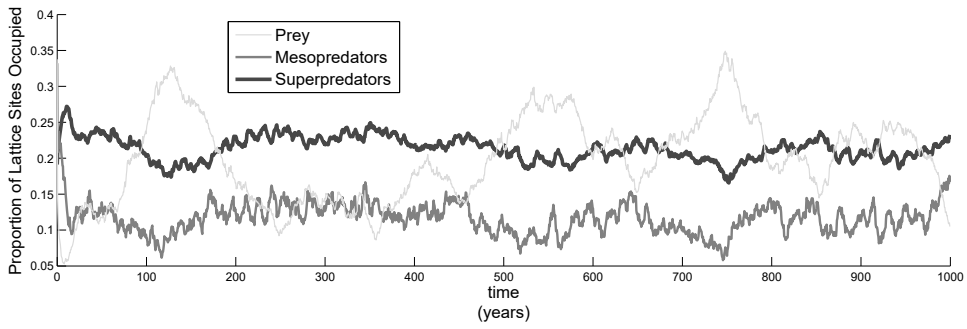
The final population values as a result of varying ν_3 are depicted in Figure 6(c). The increase in the predation rate of the cats causes the rat population to decrease. However, since the cats benefit from the consumption of rats more so than birds, a decline in the rat population also transmits to a dip in the cat population. Having both predator populations at low levels allow for an increase in the number of birds. With the increasing predation of cats, the bird

population persists at high levels because the cats maintain the rat population at small numbers and free up a good amount of lattice space for the birds to produce their offspring. This case is interesting because one would expect as the predator populations reach a low threshold having so many birds around would help the cats and rats, however our results suggest otherwise.

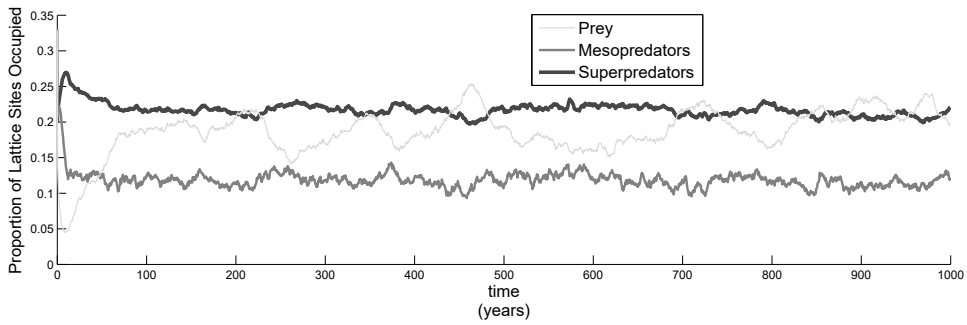
Figure 6(d) displays the final results of varying the parameter η_{31} . Above in Figure 6(c), we found that the cat population declines as it reduces the number of rats, their main source of nutrition, through predation. On the other hand, an increase in the value of η_{31} means the cats are able to attain more nutrition from the consumption of birds, so the steady decline of cats that is apparent in 6(c) becomes a moderate decrease in 6(d). The reduced population of rats still causes a significant increase in the bird population. Though, as the rat population reaches a low threshold and the cats begin to rely more on the nutrition they receive from the consumption of birds, we begin to see a sharp decline in the bird population. Although we consider cats to be opportunistic hunters that consume prey based on availability, some elements of prey switching are evident as we vary η_{31} . This is a byproduct of the spatial predation structure.

6.2 Spatial Analysis

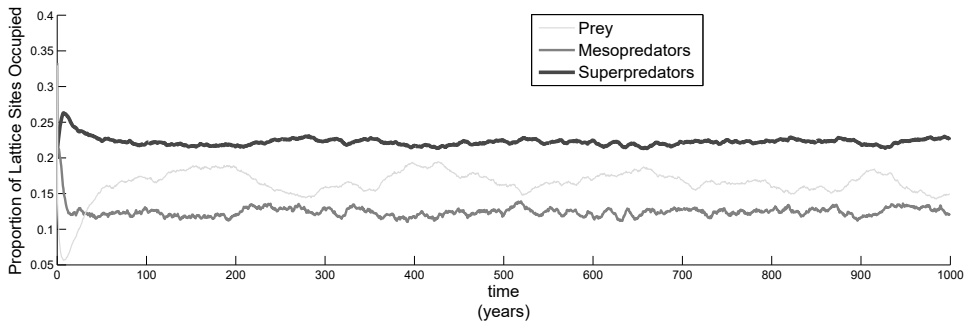
Before we examine the spatial structure resulting from the simulation, it is important to analyze the effect of lattice size on our equilibrium population. Figure 7 consists of the time series plots from simulating our system with the standard parameters on three increasing lattice sizes. All three simulations began with the same initial proportions for the initial distribution and ran



(a) 75×75 lattice



(b) 150×150 lattice



(c) 300×300 lattice

Figure 7: Simulation run with standard parameters from Table 2 (SIM values) on 75×75 (a), 150×150 (b), and 300×300 (c) lattices.

for the same amount of time. As you can see in Figure 7(a), the plot for a 75×75 grid, the prey population exhibits oscillation with a large amplitude and a long period. Quadrupling the total lattice size to 150×150 , as in Figure 7(b), decreases the amplitude and the period of the oscillations. Another quadrupling of the total lattice size to 300×300 , as in Figure 7(c), further decreases the amplitude and the period of the oscillations.

This effect on the oscillations as we increase lattice size is the result of averaging over a larger lattice. Locally, the lattice is constantly changing, but as we increase the size of the lattice we have more of these local areas that are being averaged over with the result being smaller total oscillations over the whole lattice; even though the local dynamics remain unchanged. These local dynamics lead to the local clustering present in our population map.

The population map develops a definite spatial structure over time in our simulation. The development of this spatial structure is evident in the population map snapshots of Figure 8 which represent the population over time on a 150×150 lattice. At time zero, the population is initialized to be randomly distributed on the lattice such that the prey occupy 33% of the lattice sites, the mesopredators occupy a corresponding 33% of the lattice and the superpredators occupy 20%. The remaining lattice sites are left empty. Soon after the initial distribution, at the five year mark in our simulation, the prey and mesopredator population have significantly decreased, corresponding to the sharp decline on the time-series population graphs in Figure 7. At this point the superpredator population has risen on the lattice.

As time increases the spatial structure of the lattice begins to develop. At the fifty year mark the prey have begun to form clusters, while the mesopredators form smaller clusters and the

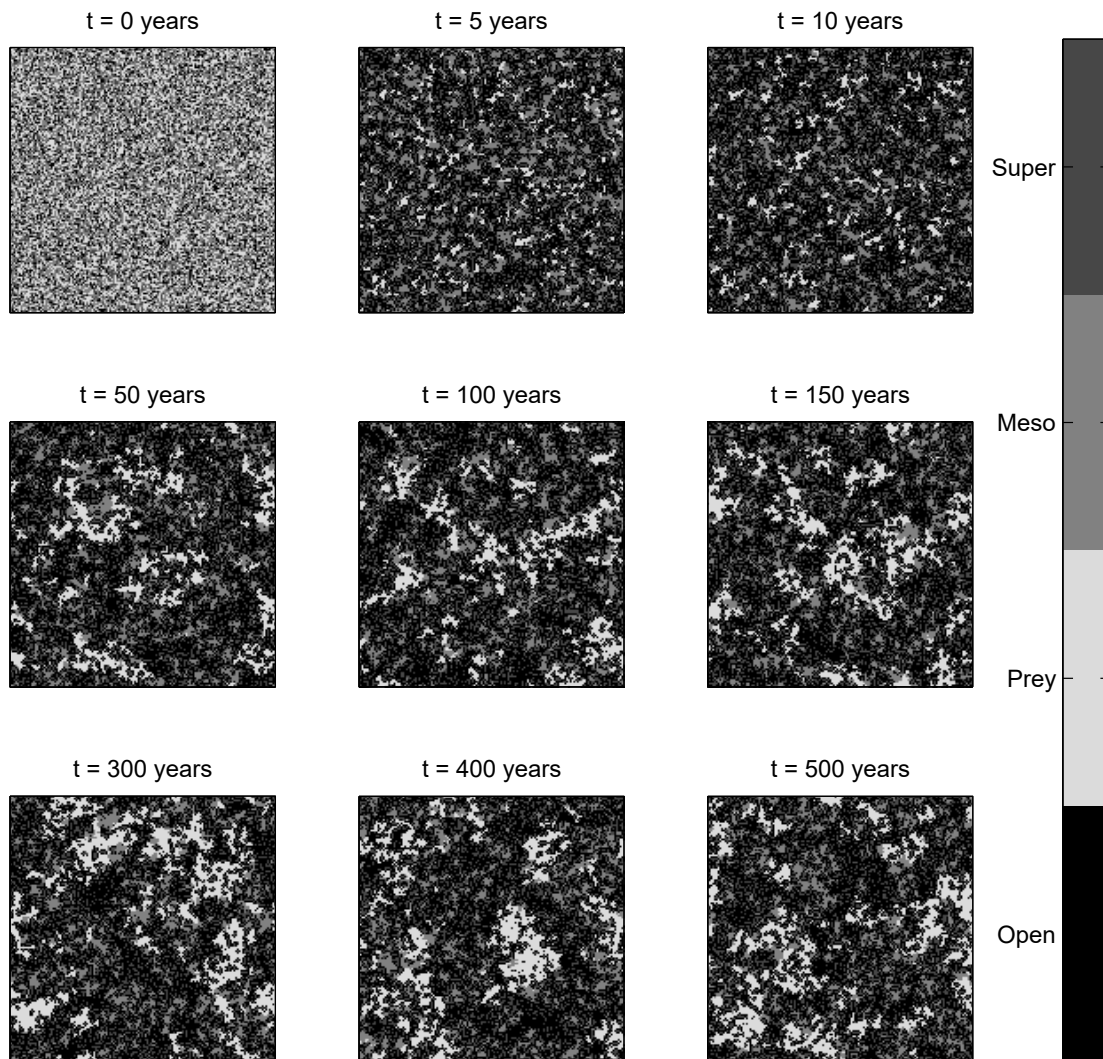


Figure 8: Snapshots of population map at various times for standard parameters on a 150×150 lattice.

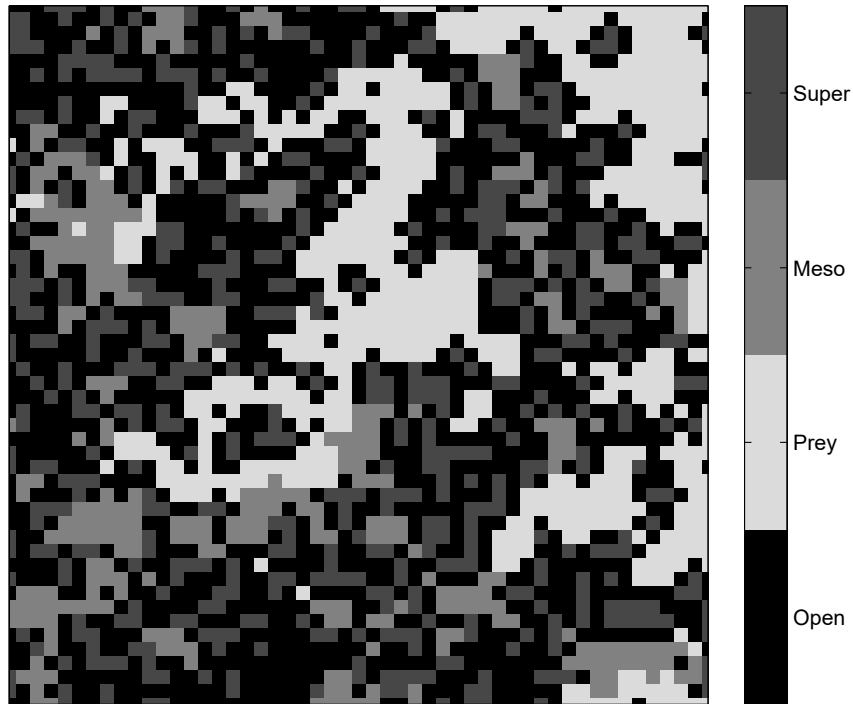


Figure 9: Close up of subset of population map at 500 years.

superpredators have become scattered. Once we have simulated until three hundred years the final spatial structure of the lattice emerges. The prey cluster in in large groups, occupying a significant portion of the lattice. The mesopredators cluster in various sized smaller groups with the larger of these groups occupying lattice sites adjacent to prey clusters. The superpredators are scattered and tend to form rings around the prey clusters and cluster marginally near mesopredator population. Figure 9 shows a close up image of the lattice and provides a better view of the various clustering and scattering phenomenon.

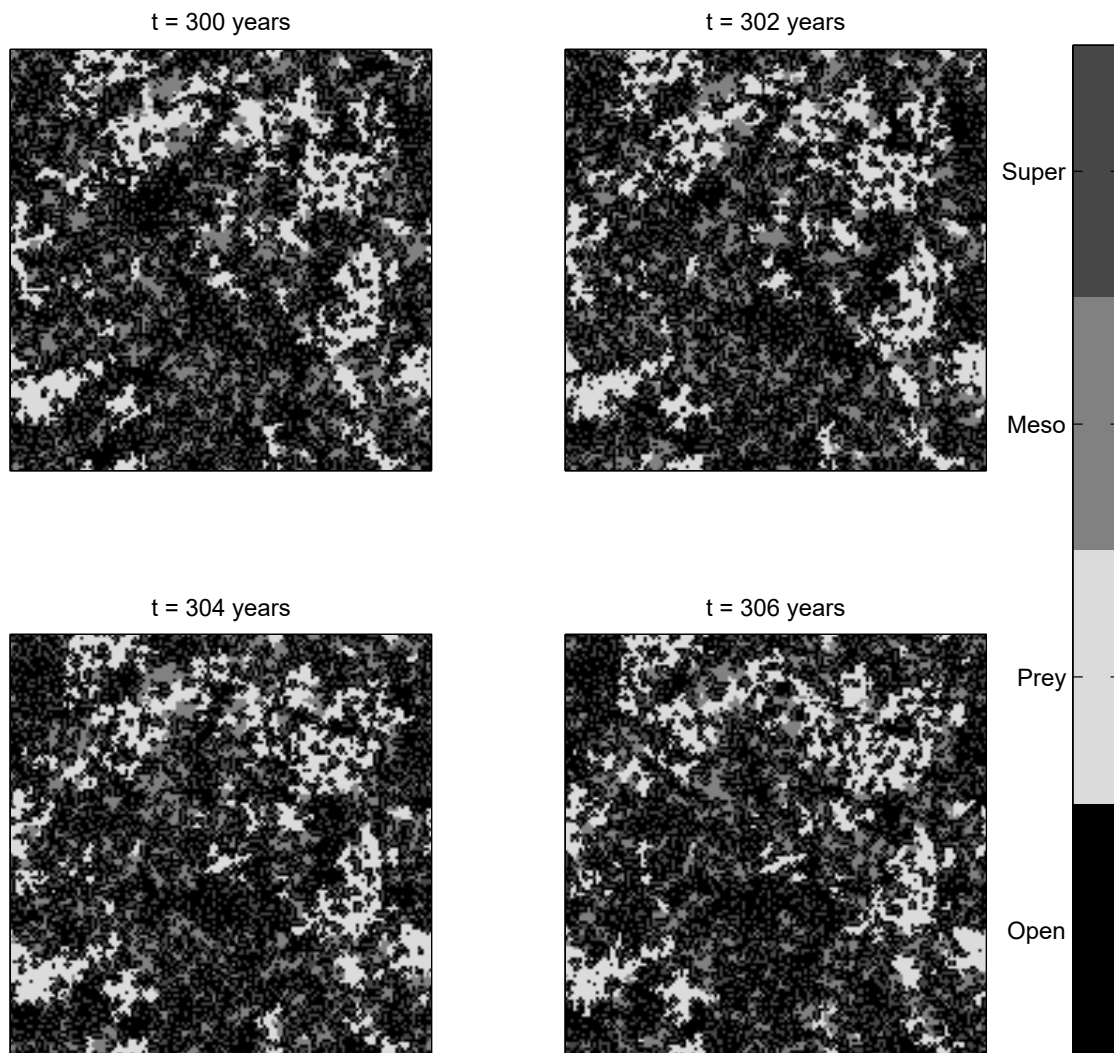


Figure 10: Snapshots of population map at every two years starting at year 300 for standard parameters.

These clustering effects demonstrate that the simulation has produced natural behavior even though such behavior was not explicitly added. The clustering of the prey is interpreted as a

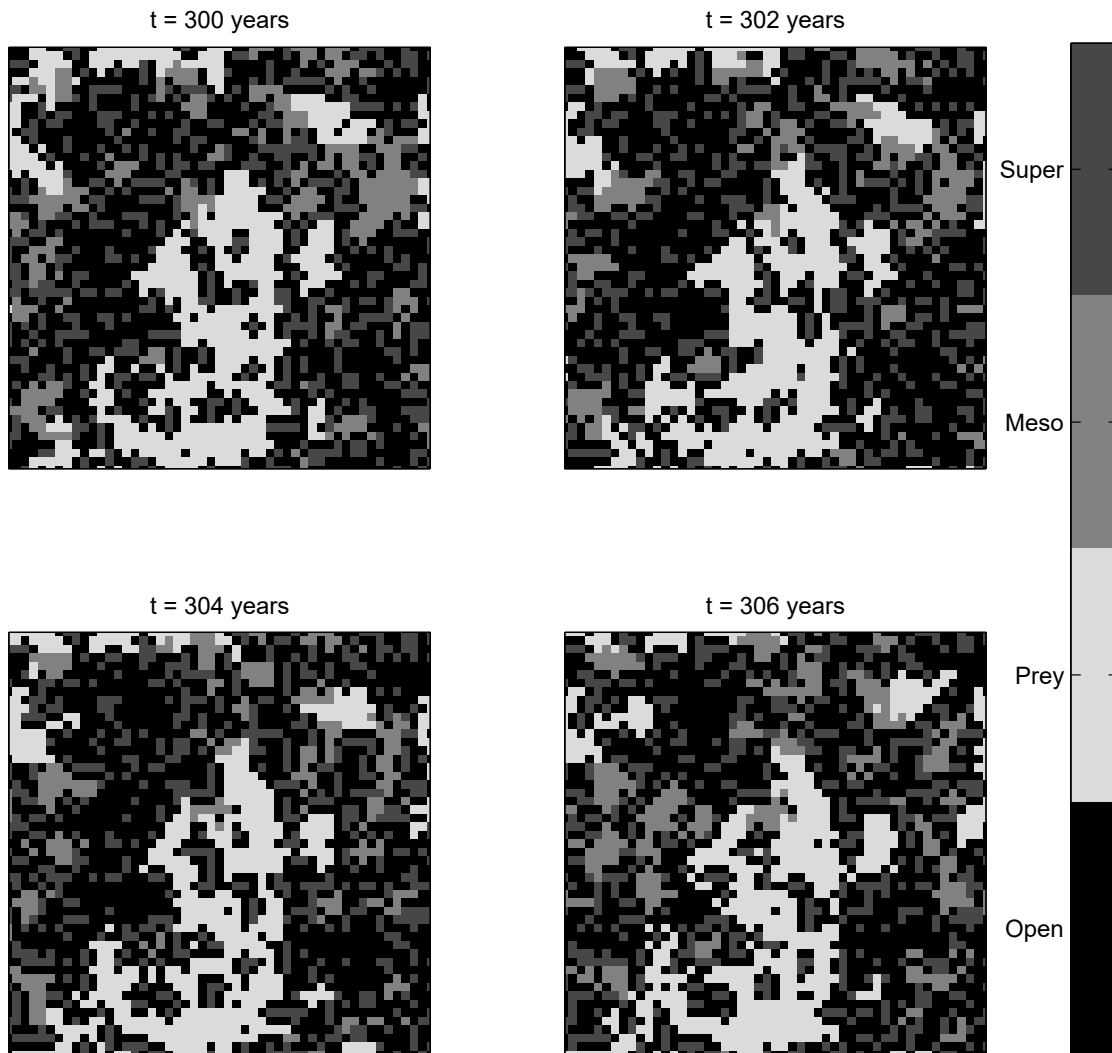


Figure 11: Close up of snapshots of population map at every two years starting at year 300 for standard parameters.

defense mechanism to protect them from their predators. The mesopredator clustering is a result of their high birth rate as they swarm through any large open areas on the lattice or through

prey clusters. In general the mesopredators tend to ‘chase’ the prey since the prey’s birth rate exceeds the predation rate of the mesopredator. In effect, the prey consume empty space on the lattice faster than the mesopredators can consume them. The superpredator scattering is a result of its lack of intrinsic birth rate, since they cannot reproduce to maintain their own clusters. The ring around prey sites results from the predation rate of the superpredator, as well as, the the low value in η_{31} . Superpredators will consume prey on the outside edge of a prey cluster but are not likely to reproduce after consumption. The small amount of clustering seen in the superpredators near the mesopredator cluster is the result of the higher η_{32} value and the mesopredator’s large birth rate. Superpredators will consume the mesopredators and will tend to wipe out a cluster due to the high availability of the mesopredator from its birth rate. These dynamic effects are illustrated in Figure 10 which displays the population map at two-year intervals.

An interesting clustering effect that can only be seen on smaller scales, as in the close up images of Figure 11, is that the prey can, in effect, kill off the superpredator. Notice that in the center of the large prey cluster depicted in Figure 11 there exist a small number of superpredators. This particular structure could only occur by the prey giving birth to new prey over time and surrounding the superpredators. Over time this superpredator population decreases until it finally dies out. This example demonstrates how superpredators are dependant upon the mesopredator population; superpredators cut off from a mesopredator cluster will eventually die out over time, even when surrounded by prey.

6.3 Comparisons and Recommendations

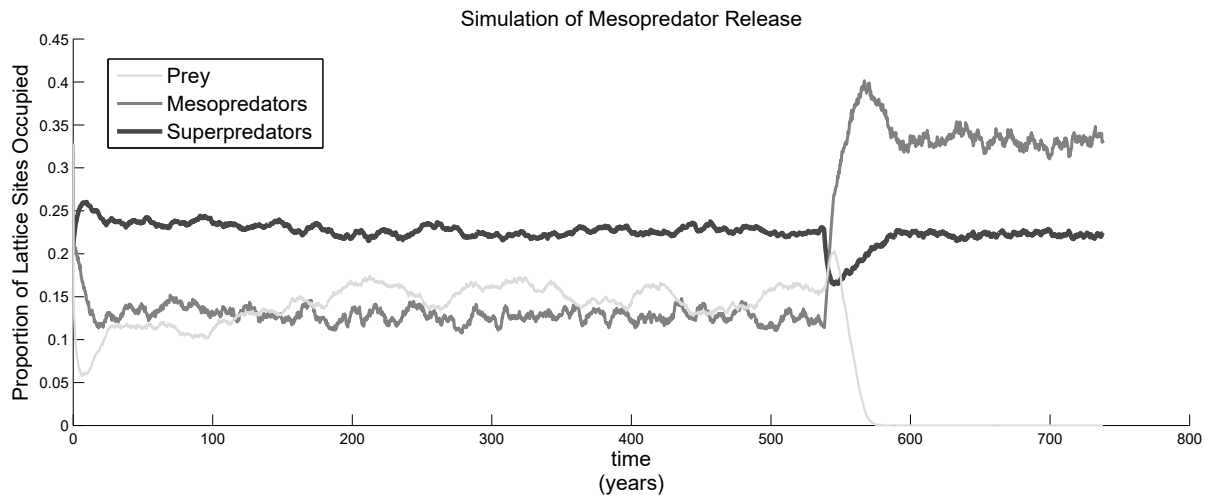


Figure 12: Time series of the Mesopredator Release with μ_3 changing from $\frac{1}{10}$ to $\frac{1}{5}$ on a 150×150 lattice.

The mesopredator release suggests that a decline in the superpredator population causes a significant rise in the mesopredator population and leads to the extinction of the prey. One of the explored control strategies for aiding endangered prey species is the removal of superpredators from the ecosystem. In many cases, this is not the optimal strategy as it may lead to an increase in smaller predators followed by the extinction of the endangered species. Previous studies [7, 14], as well as, the results of our spatial model, support the existence of this hypothesis. In our model, we developed a simulation that displays coexistence between the three species. We then increased μ_3 to simulate rapid eradication of superpredators from the ecosystem; this immediately led to an increase in the mesopredator population, and then the annihilation of the prey population (see Figure 12).

Studies by Courchamp et. al. also give rise to other scenarios of coexistence that the spatial model can reaffirm [7]. For instance, coexistence between both predators in the absence of the prey population are feasible when prey death rate or mesopredator predation rate is relatively greater than the standard parameters values that would give coexistence (see Appendix B, figures 17(c) and 19(c)). Coexistence is practicable because mesopredators are omnivorous and can survive in the absence of prey, while the superpredators maintain their population from a persistent number of mesopredators. Another interesting phenomenon is the case where the superpredators drive the mesopredators to extinction and not the prey. This occurrence can be observed in the simulation when the prey has a moderately high birth rate (see Appendix B figure 13). In essence, the mesopredators go extinct as a result of being outcompeted for space by the growing prey population, and the superpredators survive because of the availability of prey.

By introducing space to the study of superpredator-mesopredator-prey dynamics we include functional response of the predators as originally suggested and utilized by Fan et. al. [14]. The term functional response refers to the interference between predators of the same species when foraging for food; this occurrence is also known as intraspecific competition. Since foraging is a local event in our model, having two predators on adjacent sites of the lattice reduces the effectiveness of their search for food (for more explanation and pictorial understanding see Section 6.2 above).

Extinction is a threat many species face across the world, especially island bird populations. The purpose of this research was to develop a more realistic model of superpredator-

mesopredator-prey dynamics and, through analysis of the model, determine a more practical control method for the conservation of endangered prey species. The most realistic management method for maintaining the prey at high levels and the predators at relatively low levels is to control the mesopredator population (increased death rate) (see Appendix B Figures 17(c) and 18(c)).

7 Conclusion

We conclude that the inclusion of space in our model has a significant effect on the results of the model, particularly with respect to the parameters (see Appendix B). Space plays an important role in analysis of the system and its inclusion will produce nonintuitive results for varying some parameters. For example, we observed that increasing the natural birth rate of the mesopredator can have a deleterious effect on their population level; an effect that is both unexpected and unrepresented in both approximation models. The importance of space is also noted in the resulting ‘real-world’ behavior of the species in the simulation. This result, though intuitive, cannot fully be represented in the spatially-implicit mean field model or the spatially-local pair approximation model.

Furthermore, the results presented here coincide with reports from previous models. And to our knowledge, this is the first study to incorporate space into the study of superpredator-mesopredator-prey systems, which was one of the recommendations that Courchamp and collaborators mentioned in their work [7]. Finally, we *can* have a persistent population of prey solely by controlling the population of mesopredators. Also, the suppression of the superpredator has

a negative effect on the prey population.

Our recommendations for future work lie in three main areas: more inclusive, realistic simulations, biologically sound parameter values, and more precise approximation methods. We recommend that future simulations of our model look at the inclusion of heterogeneous landscapes for the species to live on. In our model, we have ignored any effect that a clustered landscape could have on our system. Simulations including non-toroidal boundary conditions, such as Dirichlet or Neuman boundary conditions, where the entire lattice could represent a single island system are also future possibilities. Since a simulation of this magnitude would possibly require an exceptionally large lattice size, we also look forward to creating a version of our simulation that can run on these lattice sizes (over 1000×1000), and possibly develop the model in a parallel environment. Our parameters need to be refined in order to see if our simulation does accurately model reality; in particular, the values for the various η parameters need further verification. The mean field and pair approximation methods do not adequately capture the complex spatial dynamics of our model and as such more accurate approximations that account for large regions of space need to be applied to the model.

8 Acknowledgements

We want to give special thanks to Dr. Carlos Castillo-Chavez for giving us the privilege and opportunity to become part of the researchers at MTBI 2007. His experience and wisdom have also become essential in our research and our academic development.

We would also like to thank Dr. David Hiebeler, Dr. Fabio Sanchez, David Murillo and

Jose Almora for all the help and knowledge they provided us in our research.

The MTBI/SUMS Summer Undergraduate Research Program is supported by The National Science Foundation (DMS-0502349), The National Security Agency (DOD-H982300710096), The Sloan Foundation, and Arizona State University.

References

- [1] Amarasekare, P. (1993). Potential impact of mammalian nest predators on endemic forest birds of Western Mauna Kea Hawaii. *Conservation Biology* 7: 316-324.
- [2] Atkinson, I. (1985). The spread of commensal species of *Rattus* to oceanic islands and their effect on islands avifaunas. In: Moors, P. (Ed.). *Conservation of Island Birds: case studies for the management of threatened island species*. ICBP technical Publication No 3. Cambridge. pp 35-81.
- [3] Atkinson, I. (1989). Introduced animals and extinctions. In: Western, D and Pearl, M(Eds.). *Conservation for the Twenty-first Century*. Oxford University Press. New York. pp 54-75.
- [4] Case, T. and Bolger, D. (1991). The role of introduced species in shaping the distribution and abundance of island reptiles. *Evolutionary Ecology* 5: 272-290.
- [5] Caswell, H. and Etter, R. (1993). Ecological interactions in: patchy environments: From patch occupancy models to cellular automata. In: Powell, T. Levin, S. and Steele, J. (Eds.). *Patch Dynamics*. Springer-Verlag. New York. pp 93-109.

- [6] Ceballos G. and Brown, J. (1995). Global patterns of mammalian diversity, endemism and endangerment. *Conservation Biology* 9: 559-568.
- [7] Courchamp, F., Langlais, M. and Sugihara, G. (1999) Cats protecting birds: modelling the mesopredator release effect. *Journal of Animal Ecology* 68: 282-292.
- [8] Cree, A., Daugherty, C. and Hay, J. (1995). Reproduction of a rare New Zealand reptile, the Tuatara *Sphenodon punctatus*, on rat-free and rat-inhabit islands. *Conservation Biology* 9: 373-383.
- [9] Crooks, K. and Soule, M. (1999). Mesopredator release and avifaunal extinctions in a fragmented system. *Nature* 400: 563-566.
- [10] Curry, R. (1985). Breeding and survival of Galapagos mockingbirds during El Niño. In: Robinson, G. and del Pino, E. (Eds.). *El Niño in the Galapagos Islands: the 1982-1983 event*. Charles Darwin Foundation. Quito. pp 449-471
- [11] Curry, R. and Grant, P. (1989). Demography of the cooperative breeding Galapagos mockingbird (*Nesomimus parvulus*) in a climatically variable environment. *Journal of Animal Ecology* 58:441-464.
- [12] Dobson, A. (1988). Restoring island ecosystems: the potential of parasite to control introduced mammals. *Conservation Biology* 2: 31-39.
- [13] Domm, S. and Messersmith, J. (1990). Feral cat eradication on a barrier reef island, Australia. *Atoll Research Bulletin* 338: 1-4.

- [14] Fan, M., Kuang, Y. and Feng, Z. (2005). Cats protecting birds revisited. *Bulletin of Mathematical Biology* 67: 1081-1106.
- [15] Gehrt, S. and Clark, W. (2003). Raccoons, coyotes, and reflections on the mesopredator release hypothesis. *Wildlife Society Bulletin* 31: 836-842.
- [16] Global Invasive Species Database. <http://www.issg.org/database>.
- [17] Iverson, J. (1978). The impact of feral cats and dogs on populations of the west Indian rock iguana, *Cyclura carinata*. *Biological Conservation* 14: 63-73.
- [18] King W. (1985). Island birds: will the future repeat the past? In: Moors, P. (Ed.). *Conservation of Island Birds: case studies for the management of threatened island species*. ICBP technical Publication No 3. Cambridge. pp 3-15.
- [19] Monteiro, L. Ramos, J. and Furness, R. (1996). Past and present status and conservation of the seabirds breeding in the Azores Archipelago. *Biological Conservation* 78: 319-328.
- [20] Morozov, A., Petrovskii, S. and Li, B. (2006). Spatiotemporal complexity of the patchy invasion in a predator-prey system with the Allee effect. *Journal of theoretical Biology* 238: 18-35
- [21] Ogan, C. and Jurek, R. (1997). Biology and Ecology of feral, free-roaming, and stray cats. In: Harris, E. and Ogan, C. (Eds.). *Mesocarnivores of northern California: biology, management, and survey techniques, workshop manual*. The Wildlife Society, California North Coast Chapter. Arcata. pp 87-92.

- [22] Rodriguez-Estrella, R., Arnaud, G., Cardenas, S. and Rodriguez, A. (1991). Predation by feral cats on birds at Isla Socorro. *Western Birds* 22: 141-143.
- [23] Rogers, C. and Caro, M. (1998). Song sparrows, top carnivores and nest predation: A test of the mesopredator release hypothesis. *Oecologia* 116: 227-233.
- [24] Rohani, P., Lewis, T., Grunbaum, D. and Ruxton, G. (1997). Spatial self organization in ecology: pretty patterns or robust reality? *Trends in Ecology and Evolution* 12: 70-74
- [25] Sala, O., Chapin, F., Armesto, J., Berlow, E., Bloomfield, J., Dirzo, R., Huber-Sanwald, E., Huenneke, L., Jackson, R., Kinzig, A., Leemans, R., Lodge, D., Mooney, H., Oesterheld, M., Poff, N., Sykes, M., Walker, B., Walker, M. and Wall, D. (2000). Global biodiversity scenarios for the year 2100. *Science* 287: 1770-1774.
- [26] Schmidt, K. (2003). Nest predation and population declines in Illionis songbirds: A case for mesopredator effects. *Conservation Biology* 17: 1141-1150.
- [27] Schmidt, P., Lopez, R. and Collier, B. (2007). Survival, Fecundity, and Movements of Free-Roaming Cats. *Journal of Wildlife management* 71: 915-919.
- [28] Seto, N. and Conant, S. (1996). The effects of rat (*Rattus rattus*) predation on the reproductive success of the Bonin Petrel (*Pterodroma hypoleuca*) on Midway Atoll. *Colonial Waterbirds* 19: 171-185.

- [29] Soule, M., Bolger, D., Alberts, A. Wright, J. Sorice, M. and Hill, S. (1988). Reconstructed dynamics of rapid extinctions of chaparral-requiring birds in urban habitat islands. *Conservation Biology* 2: 75-92.
- [30] Spencer, P. (1991). Evidence of predation by a feral cat *Felis catus* carnivora felidae on an isolated rock-wallaby colony in tropical queensland australia. *Australian Mammalogy* 14: 143-144.
- [31] Tamarin, R. and Malecha, S. (1972). Reproductive parameters in *Rattus rattus* and *Rattus exulans* of Hawaii, 1968 to 1970. *Journal of Mammalogy* 53: 513-528
- [32] Tidemann, C., Yorkston, H. and Russack, A. (1994). The diet of cats, *Felis catus*, on Christmas Island, Indian Ocean. *Wildlife Research* 21: 279-286.
- [33] Wilson, W., Harrison, S., Hastings, A. and McCann, K. (1999). Exploring stable pattern formation in models of tussock moth populations. *Journal of animal ecology* 68:94-107
- [34] Wilson, W., Morris, W. and Bronstein, J. (2003). Coexistence of mutualists and exploiters in spatial landscapes. *Ecological monographs* 73: 397-413

A Appendix

This Appendix lists the nine pair approximation equations:

$$\begin{aligned}
\frac{dP[00]}{dt} &= 2P[01] \left(\mu_1 + \frac{3}{4}\nu_2 Q_{2|1} (1 - \eta_2) + \frac{3}{4}\nu_3 Q_{3|1} (1 - \eta_{31}) \right) \\
&\quad + 2P[02] \left(\mu_2 + \frac{3}{4}\nu_3 Q_{3|2} (1 - \eta_{32}) + 2P[03]\mu_3 \right) \\
&\quad - 2P[00] \left(\frac{3}{4}\phi_1 Q_{1|0} + \frac{3}{4}\phi_2 Q_{2|0} + \frac{3}{4}\phi_3 Q_{3|0} \right)
\end{aligned} \tag{11}$$

$$\begin{aligned}
\frac{dP[01]}{dt} &= P[00] \frac{3}{4}\phi_1 Q_{1|0} + P[11] \left(\mu_1 + \frac{3}{4}\nu_2 Q_{2|1} (1 - \eta_2) + \frac{3}{4}\nu_3 Q_{3|1} (1 - \eta_{31}) \right) \\
&\quad + P[12] \left(\mu_2 + \frac{3}{4}\nu_3 Q_{3|2} (1 - \eta_{32}) \right) + P[13]\mu_3 \\
&\quad - P[01] \left(\mu_1 + \phi_1 \left(\frac{3}{4}Q_{1|0} + \frac{1}{4} \right) + \frac{3}{4}\phi_2 Q_{2|0} + \frac{3}{4}\phi_3 Q_{3|0} + \frac{3}{4}\nu_2 Q_{2|1} + \frac{3}{4}\nu_3 Q_{3|1} \right)
\end{aligned} \tag{12}$$

$$\begin{aligned}
\frac{dP[02]}{dt} &= P[00] \frac{3}{4}\phi_2 Q_{2|0} + P[12] \left(\mu_1 + \nu_2 \left(\frac{3}{4}Q_{2|1} + \frac{1}{4} \right) (1 - \eta_2) + \frac{3}{4}\nu_3 Q_{3|1} (1 - \eta_{31}) \right) \\
&\quad + P[22] \left(\mu_2 + \frac{3}{4}\nu_3 Q_{3|2} (1 - \eta_{32}) \right) + P[23]\mu_3 + P[01] \frac{3}{4}Q_{2|1}\nu_2\eta_2 \\
&\quad - P[02] \left(\mu_2 + \frac{3}{4}\nu_3 Q_{3|2} + \frac{3}{4}\phi_1 Q_{1|0} + \phi_2 \left(\frac{3}{4}Q_{2|0} + \frac{1}{4} \right) + \frac{3}{4}\phi_3 Q_{3|0} \right)
\end{aligned} \tag{13}$$

$$\begin{aligned}
\frac{dP[03]}{dt} &= P[00] \frac{3}{4}\phi_3 Q_{3|0} + P[01] \frac{3}{4}Q_{3|1}\nu_3\eta_{31} + P[02] \frac{3}{4}Q_{3|2}\nu_3\eta_{32} \\
&\quad + P[13] \left(\mu_1 + \frac{3}{4}\nu_2 Q_{2|1} (1 - \eta_2) + \nu_3 \left(\frac{3}{4}Q_{3|1} + \frac{1}{4} \right) (1 - \eta_{31}) \right) \\
&\quad + P[23] \left(\mu_2 + \nu_3 \left(\frac{3}{4}Q_{3|2} + \frac{1}{4} \right) (1 - \eta_{32}) \right) + P[33]\mu_3 \\
&\quad - P[03] \left(\mu_3 + \frac{3}{4}\phi_1 Q_{1|0} + \frac{3}{4}\phi_2 Q_{2|0} + \phi_3 \left(\frac{3}{4}Q_{3|0} + \frac{1}{4} \right) \right)
\end{aligned} \tag{14}$$

$$\begin{aligned}\frac{dP[11]}{dt} &= 2P[01]\phi_1 \left(\frac{3}{4}Q_{1|0} + \frac{1}{4} \right) \\ &\quad - 2P[11] \left(\mu_1 + \frac{3}{4}\nu_2Q_{2|1} + \frac{3}{4}\nu_3Q_{3|1} \right)\end{aligned}\tag{15}$$

$$\begin{aligned}\frac{dP[12]}{dt} &= P[02]\frac{3}{4}\phi_1Q_{1|0} + P[01]\frac{3}{4}\phi_2Q_{2|0} \\ &\quad + P[11]\frac{3}{4}\nu_2\eta_2Q_{21} \\ &\quad - P[12] \left(\mu_1 + \mu_2 + \nu_2 \left(\frac{3}{4}Q_{2|1} + \frac{1}{4} \right) + \nu_3 \left(\frac{3}{4}Q_{3|1} + \frac{3}{4}Q_{3|2} \right) \right)\end{aligned}\tag{16}$$

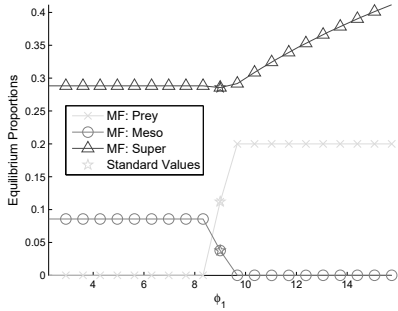
$$\begin{aligned}\frac{dP[13]}{dt} &= P[03]\frac{3}{4}\phi_1Q_{1|0} + P[01]\frac{3}{4}\phi_3Q_{3|0} \\ &\quad + P[11]\frac{3}{4}\nu_3\eta_{31}Q_{3|1} + P[12]\frac{3}{4}\nu_3\eta_{32}Q_{3|2} \\ &\quad - P[13] \left(\mu_1 + \mu_3 + \frac{3}{4}\nu_2Q_{2|1} + \nu_3 \left(\frac{3}{4}Q_{3|1} + \frac{1}{4} \right) \right)\end{aligned}\tag{17}$$

$$\begin{aligned}\frac{dP[22]}{dt} &= 2P[02]\phi_2 \left(\frac{3}{4}Q_{2|0} + \frac{1}{4} \right) \\ &\quad + 2P[12]\nu_2\eta_2 \left(\frac{3}{4}Q_{2|1} + \frac{1}{4} \right) \\ &\quad - 2P[22] \left(\mu_2 + \frac{3}{4}\nu_3Q_{3|2} \right)\end{aligned}\tag{18}$$

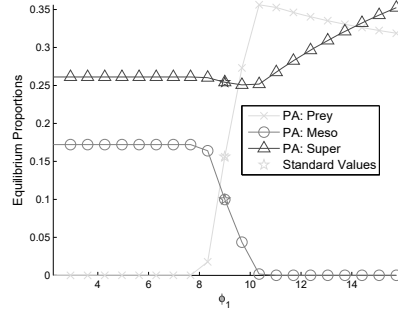
$$\begin{aligned}\frac{dP[23]}{dt} &= P[03]\frac{3}{4}\phi_2Q_{2|0} + P[02]\frac{3}{4}\phi_3Q_{3|0} \\ &\quad + P[13]\frac{3}{4}\nu_2\eta_2Q_{2|1} + P[12]\frac{3}{4}\nu_3\eta_{31}Q_{3|1} + P[22]\frac{3}{4}\nu_3\eta_{32}Q_{3|2} \\ &\quad - P[23] \left(\mu_2 + \mu_3 + \nu_3 \left(\frac{3}{4}Q_{3|2} + \frac{1}{4} \right) \right)\end{aligned}\tag{19}$$

B Appendix

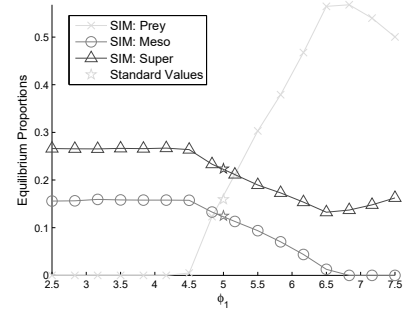
This is a list of figures that depict the change in the mean field approximation, pair approximation and the simulation when changing our eleven parameters.



(a)

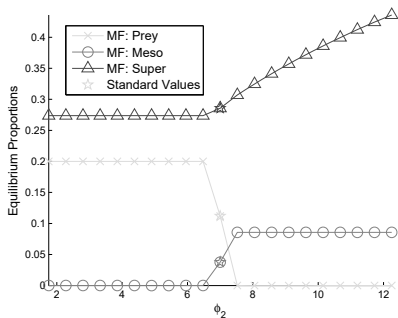


(b)

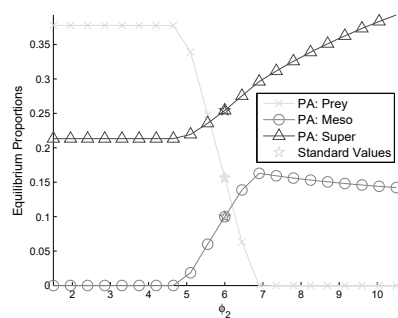


(c)

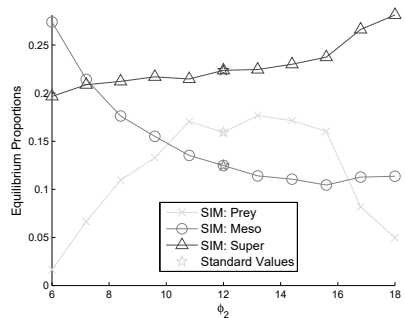
Figure 13: Plots of Mean Field Model (a), Pair Approximation (b) and Simulation Equilibria (c) versus ϕ_1



(a)

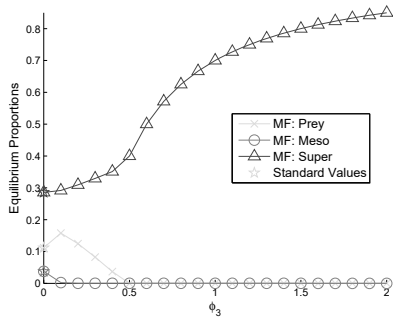


(b)

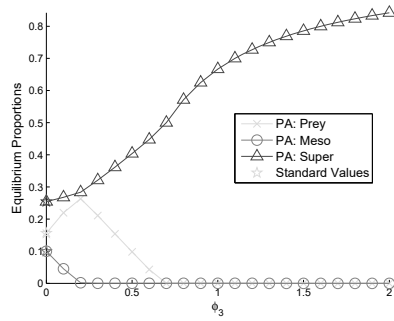


(c)

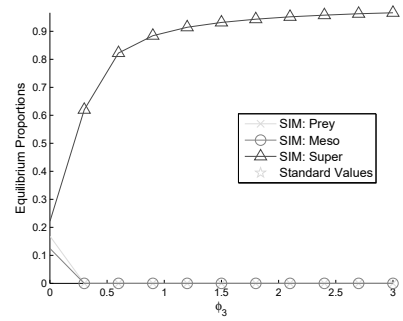
Figure 14: Plots of Mean Field Model (a), Pair Approximation (b) and Simulation Equilibria (c) versus ϕ_2



(a)

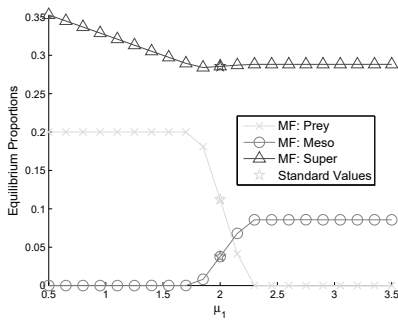


(b)

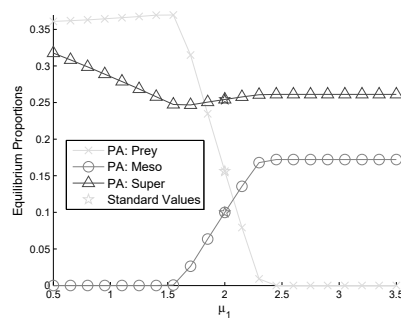


(c)

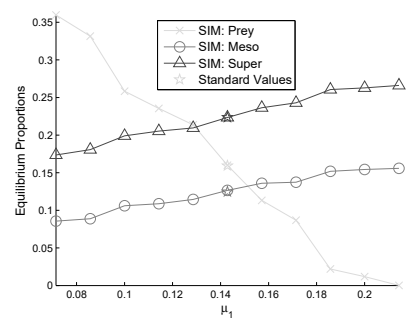
Figure 15: Plots of Mean Field Model (a), Pair Approximation (b) and Simulation Equilibria (c) versus ϕ_3



(a)

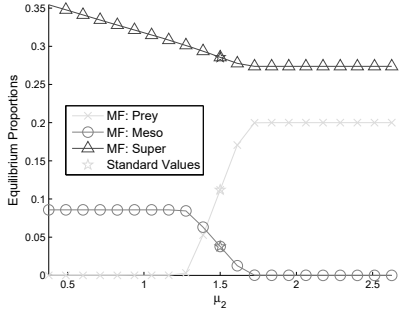


(b)

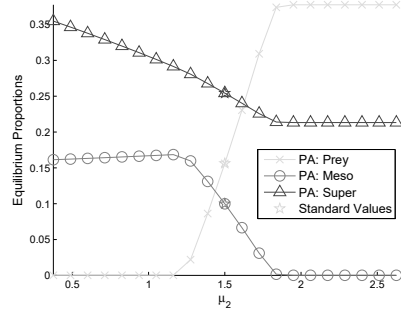


(c)

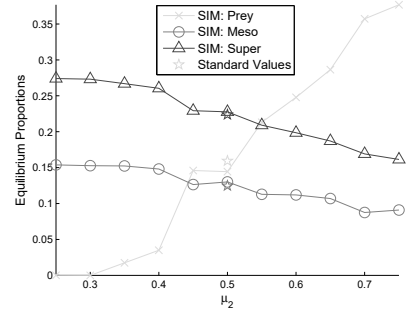
Figure 16: Plots of Mean Field Model (a), Pair Approximation (b) and Simulation Equilibria (c) versus μ_1



(a)

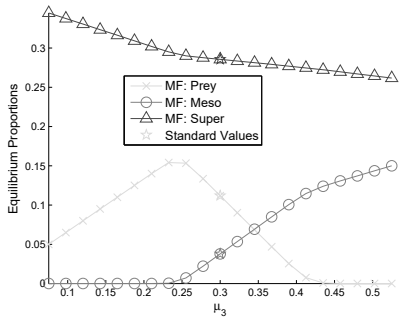


(b)

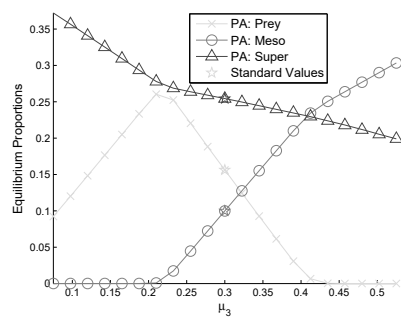


(c)

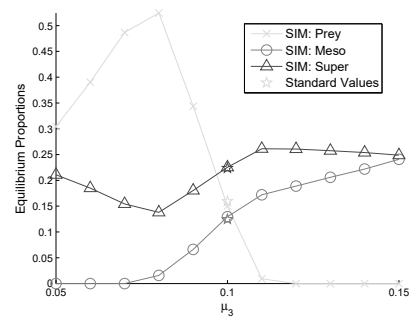
Figure 17: Plots of Mean Field Model (a), Pair Approximation (b) and Simulation Equilibria (c) versus μ_2



(a)

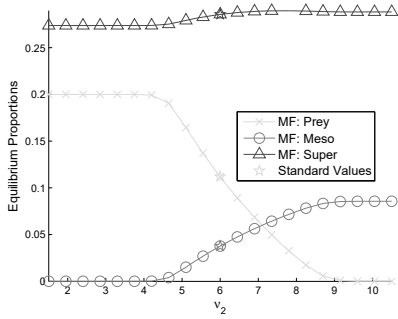


(b)

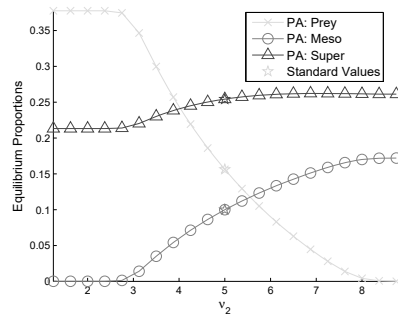


(c)

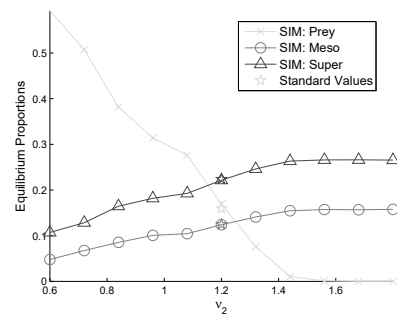
Figure 18: Plots of Mean Field Model (a), Pair Approximation (b) and Simulation Equilibria (c) versus μ_3



(a)

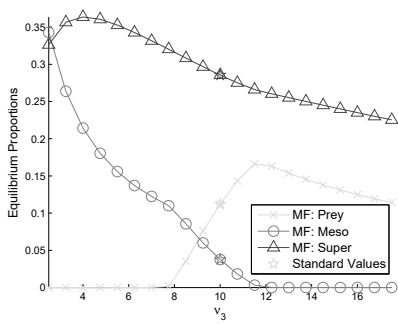


(b)

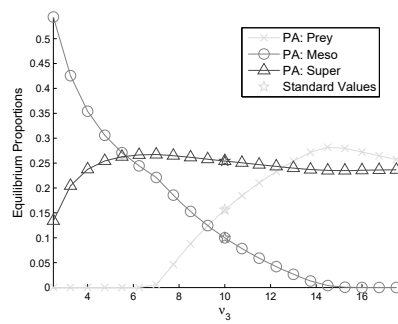


(c)

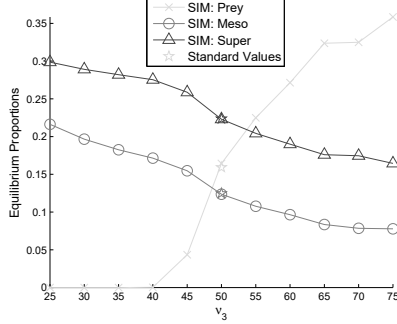
Figure 19: Plots of Mean Field Model (a), Pair Approximation (b) and Simulation Equilibria (c) versus ν_2



(a)

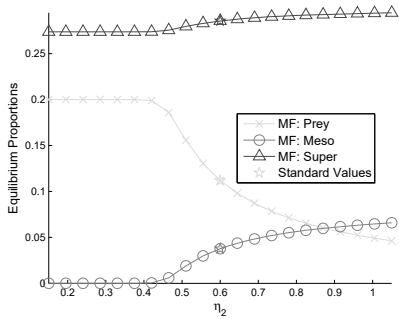


(b)

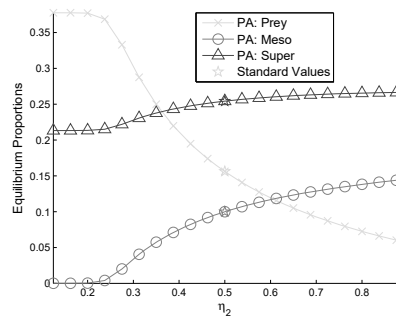


(c)

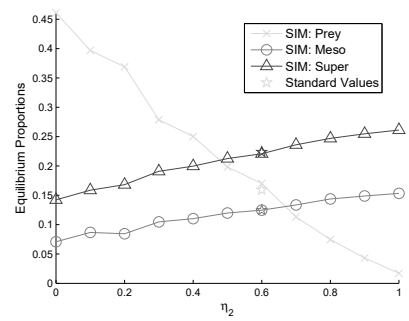
Figure 20: Plots of Mean Field Model (a), Pair Approximation (b) and Simulation Equilibria (c) versus ν_3



(a)

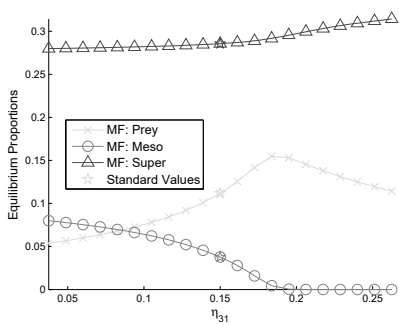


(b)

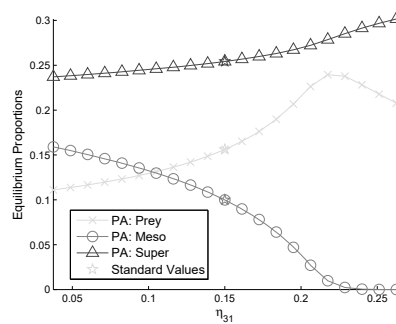


(c)

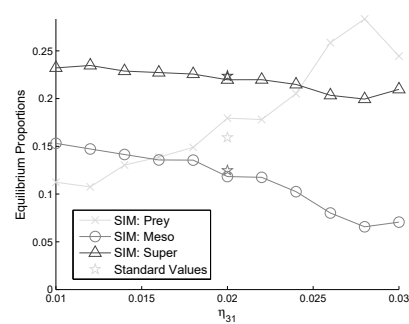
Figure 21: Plots of Mean Field Model (a), Pair Approximation (b) and Simulation Equilibria (c) versus η_2



(a)

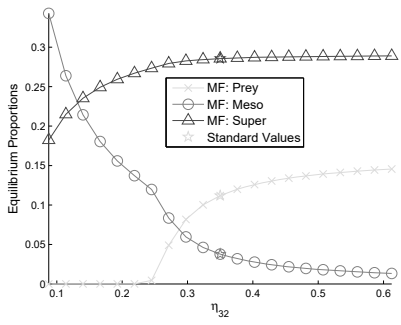


(b)

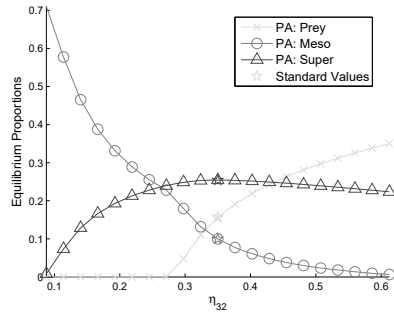


(c)

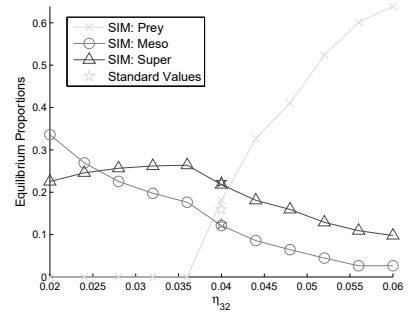
Figure 22: Plots of Mean Field Model (a), Pair Approximation (b) and Simulation Equilibria (c) versus η_{31}



(a)



(b)



(c)

Figure 23: Plots of Mean Field Model (a), Pair Approximation (b) and Simulation Equilibria (c) versus η_{32}